Extension of the Life and Enhancement of the Energy Density of Maintenance-Free Lead/Acid Batteries

by

Roland De Marco and Janine Jones

School of Applied Chemistry, Curtin University of Technology

Final Report for Project B23II (December 1997 to November 1998)

December 1998

EXECUTIVE SUMMARY

The second year of Project B23 involved a study of the beneficial effects of grid etching in caustic soda on the performance of maintenance-free lead/acid batteries using a long term charge/discharge cycling regime that simulates the real life operation of batteries (i.e., Australian Standard Traction Battery Test). Seven treated and seven untreated cells (each employing one positive and two negative plates) have been subjected to the Australian Standard Traction Battery test. Discharge capacity data demonstrated that grid etching in caustic soda has no effect on the behaviour of batteries in the early stages of cycling; however, the treatment reduces the decline in discharge capacity by 33% in the later stages of cycling. Respectively, it has been found that control and grid etched maintenance-free lead/acid batteries take approximately 110 and 130 cycles to reach 50% of initial discharge capacity. This finding represents an 18% improvement in the long-term endurance of maintenance-free batteries fabricated using grids etched in caustic soda.

All failed cells were subjected to a tear down analysis using scanning electron microscopy (SEM) and X-ray diffraction (XRD). The results of battery autopsies demonstrated that the main cause of battery failure is grid corrosion, as evidenced by a thick underlayer of an insulator (possibly lead sulfate or lead monoxide) in the corrosion layers of positive plates at the end of cycling, along with the absence of sulfation of active materials in failed positive plates.

Several dismantled cells were also examined using electron probe microanalysis (EPMA) to identify the corrosion layer of failed positive plates. The results of EPMA analyses have shown that grid etching circumvents the problem of extensive grid corrosion that leads to the formation of an insulating underlayer deposit of lead sulfate in the grid corrosion layers of failed battery plates. This advantage resides undoubtedly in the ability of the grid etching procedure to promote good adhesion between the active material and the clean grid surface.

Environmental scanning electron microscopy (ESEM), a technique that permits high resolution imaging of wet samples, has been used to study the morphological changes associated with the etching of grids in sodium hydroxide under as close as practicable to natural conditions (i.e., wet samples, straight out of solution, are mounted and examined in the ESEM). The results demonstrated that non-antimonial battery grids possess crystalline deposits of detrimental hydrocerussite, and this deleterious species is removed completely by etching in sodium hydroxide. This corroborates unequivocally the effectiveness of the grid etching procedure.

Miniaturised lead/acid battery electrodes have been designed for a novel and fundamental investigation of the electrochemistry of the lead/acid battery system using electrochemical impedance spectroscopy (EIS). Preliminary EIS data have shown that miniaturised lead battery electrodes yield an idealised EIS response in battery electrolyte (i.e., charge transfer and diffusional processes are clearly resolved), demonstrating the applicability of EIS to fundamental studies of the electrochemistry of lead/acid batteries.

It is evident that grid etching in sodium hydroxide ameliorates the detrimental influence of hydrocerussite on grid corrosion and its concomitant effect on battery durability. It is emerging that the enhancement in battery performance is less pronounced than that observed with an accelerated charge/discharge cycling regime in the 1st year of Project B23. This is expected as accelerated battery testing, in Year 1, was undertaken in order to accentuate the beneficial effects of grid etching in sodium hydroxide.

1 Introduction

1.1 Review of Previous Work

Previous work by De Marco and co-workers (1997) in the first year of Project B23 explored the use of grid etching in sodium hydroxide as a means of obviating the detrimental effects of grid hydrocerussite on battery performance (De Marco, 1997). In addition, the mechanism of premature capacity loss in maintenance-free batteries was investigated using a wide range of diagnostic tools, i.e., scanning electron microscopy (SEM), X-ray diffraction (XRD) and X-ray photoelectron spectroscopy (XPS).

Preliminary battery testing results using an artificial cycling regime that was designed to accentuate the advantages of grid etching in sodium hydroxide (De Marco and Jones, May 1997) demonstrated that it is necessary to also compress plates between absorptive glass mats in order to preserve the structural integrity of active materials, and realise the full potential of the new plate preparation process. It was shown using the cycling data for twelve treated and twelve untreated 2 V cells that grid etching in sodium hydroxide enhances the durability of maintenance-free lead/acid batteries by approximately 200%.

The active materials and corrosion layers of lead/acid battery plates have been characterised at various stages of cycling using SEM, XRD and XPS (De Marco and Jones, November 1997), and the results verified the central hypothesis of Project B23, i.e., removal of hydrocerussite-induced α-PbO by sodium hydroxide etching of grids extends the life of maintenance-free lead/acid batteries. The SEM and XRD results confirmed that the rapid capacity loss for non-antimonial batteries in the early stages of cycling (i.e., < 10 cycles) is attributable to the formation of an underlayer deposit of insulating α-PbO in the corrosion layer, and the slow decline in discharge capacity in the latter stages of cycling is due to the sluggish process of sulfation that leads to passivation of the active material. Significantly, the XPS findings identified unambiguously that insulating α-PbO is formed in the corrosion layer of an untreated plate subjected to 6 charge/discharge cycles. This represents an unequivocal elucidation of the mechanism for premature capacity loss in maintenance-free lead/acid batteries, and a scientific article

on this topic has been drafted for submission to the Journal of Applied Electrochemistry in late January or early February.

1.2 Project Goals

Although the origin of premature capacity loss in non-antimonial lead/acid batteries has been studied in detail, there have been no successful attempts to develop a remedy that extends the life of maintenance-free batteries. The first year of Project B23 confirmed the benefits of grid etching in sodium hydroxide as a means of circumventing the detrimental effects of grid hydrocerussite on battery performance by using a cycling regime that accelerated the rate of capacity loss, exemplifying and clearly establishing the effect(s) of the grid pretreatment. The second year of Project B23 involved a corroboration of the efficacy of the new battery production process by using a charge/discharge regime that simulates the real life operation of batteries, i.e., Australian Standard Traction Battery test.

1.3 Methodology

1.3.1 Grid Etching

Previous surface analyses of humidified grids that had been etched in 10 %(w/v) (De Marco, 1992) demonstrated that detrimental $2PbCO_3.Pb(OH)_2$) is removed completely through dissolution in caustic soda. Consequently, battery grids were soaked in a 10 %(w/v) sodium hydroxide solution for 15 minutes prior to plate pasting to remove grid hydrocerussite.

1.3.2 Preparation of Pasted Plates

Positive plates were prepared using the paste formula given in Table 1 (Manders et al., 1994). Barton-pot leady oxide obtained from the New South Wales plant of GNB Battery Technologies and Analytical Reagent Grade sulfuric acid (BDH, AnalaR) were used in the preparation of the paste. The paste mixing procedure entailed the addition of five separate 50 mL quantities of ultra-high-purity water to the nominal quantity of dry ingredients (i.e., leady oxide, fibre and carboxymethyl cellulose) with mixing for 2 minutes after each addition. Acid was then added to the mixture (four separate additions

of 33 mL), and the paste was mixed for 2 minutes after each addition. Finally, the remainder of the water was added to the paste, and its density was recorded after 2 minutes of mixing by measuring the volume of water displaced by 100 g of paste. The paste was then applied by hand to lead-calcium-tin grids that are commonly used in the manufacture of GNB Powersafe batteries.

Table 1. Paste formula for the preparation of positive plates.

Component	Positive paste
Leady oxide (kg)	2
Fibre (g)	0.6
Carboxymethyl cellulose (g)	5
1.40 sp. gr. H_2SO_4 (mL)	132
Water (mL)	300
Acid-to-oxide ratio (wt.%)	4.7
Paste density (g mL^{-1})	4.6-4.7

The sodium hydroxide etched and cureless paste plates were subjected to pressing in order to dry and improve the integrity of the active material. The pressing of plates entailed the stacking of four lead bricks (each weighing 11 kg) on top of six plates that were individually wrapped in one absorptive glass mat separator and sandwiched between two metal plates. The battery plates were pressed for forty five minutes before replacing the glass mat separators with fresh ones, and pressing for another forty five minutes.

1.3.3 Assembly of 2 V Cells

The cureless plates were assembled into 2 V cells comprising one positive plate surrounded by 2 negative plates. The cured negative plates were produced in the factory of GNB Battery Technologies using a paste recipe and curing conditions similar to those described elsewhere by Manders et al. (1994). Note that the alloy composition of GNB negative grids is identical to that of their positives. The positive and negative plates were separated from each other using only absorptive glass-fibre separators (approximately 3 mm thick) manufactured by GNB Battery Technologies, and the cells were placed in

GNB Powersafe battery containers. The plates were formed in 1.2 L of 1.07 sp. gr. H_2SO_4 using a constant current of 5 A for 6 hours, and then rested at open circuit for 1 hour to allow the sulfuric acid depleted diffusion layers of the pores to be replenished by the permeation of fresh electrolyte. The charge/rest period was repeated, followed by a final charge at 5 A for 6 hours. After formation, the sulfuric acid and separators were discarded, and the cells were reassembled and filled with 1.3 L of 1.270 sp. gr. H_2SO_4. Note that in all cases the electrolyte-to-plate material ratio of the cells was 4.3 mL per g.

1.3.4 Australian Standard Traction Battery Test

The durability of 2 V cells according to the Australian Standard Traction Battery Test was assessed by employing a Digatron BTS-500 computerised charge/discharge unit (Digatron GmbH, Germany) to undertake repetitive charge/discharge cycling according to the following scheme: (i) initial charging at 0.84 A up to 2.55 V, followed by a 1 hour pause; (ii) discharging at 0.84 A down to 1.70 V; (iii) charging at 0.84 A until the charge capacity was 105% of the discharge capacity obtained in step ii, followed by a 1 hour pause; (iv) steps ii and iii were repeated for a total number of 10 cycles; (v) discharging at 1.05 A for 3 hours; (vi) charging at 1.05 A for 9 hours; (vii) steps v and vi were repeated for a total number of 50 cycles; (viii) steps ii to vii were repeated until the discharge capacity fell below 80% of the 5-hour rated capacity (i.e., C_5), at which point the battery was deemed to have failed.

1.3.5 Autopsies of Cells

The failed cells were dismantled, and the positive plates were rinsed in distilled water followed by drying at 50 ^{o}C for 24 hours. The wet positive plates and glass separators were inspected manually to ascertain if active material shedding was a significant cause of cell failure. Finally, the active material of dry positive plates was analysed by XRD using a Kristalloflex Siemens D500 X-ray diffractometer fitted with a Cu Kα X-ray tube that was operated at an accelerating voltage of 20 kV and a beam current of 30 mA.

The grid corrosion layers of epoxy mounted, polished cross sections of positive plates were examined by SEM using a Phillips XL30 electron microscope operated at an

accelerating voltage of 25kV, and a spot size setting of 4. EPMA studies of corrosion layers were performed using a JEOL 6400 electron microscope equipped with three JEOL wavelength dispersive spectrometers and a Deben automated stage that was controlled by Moran Scientific Chemical Imaging software. The EPMA was operated under the following conditions: accelerating voltage of 25 kV; beam current of 10 - 15 nA; analysis grid of 128 x 128 point; each point was counted for 50 ms. The specimens were ground successively on 500, 1,000 and 1,200 grit emery paper using a water lubricant and a Struers Dap-V disc polisher that was rotated at 300 revolutions per minute. After grinding, the specimens were polished successively on Struers DP-Spray, P diamond sprays (3 and 1 micron) that had been applied to DP-Nap and DP-Mol felt pad discs using a rotation speed of 300 revolutions per minute and the Struers DP-lubricant Red.

1.3.6 Environmental Scanning Electron Microscopy (ESEM)

ESEM work was undertaken using the Electroscan ESEM(S)E-3 instrument available at the electron microscopy centre at The University of Western Australia. An accelerating voltage of 30 kV and a spot size of 40 were employed in the measurement of all images. The chamber pressure in the ESEM is 1.2 torr.

1.3.7 Electrochemical Impedance Spectroscopy (EIS)

EIS measurements were undertaken using an electrochemical impedance analyser (EG & G instruments model 6310) that was interfaced to a Radiometer Copenhagen Research pH meter (Model PHM84). A frequency range of 10 mHz to 100 kHz, and an AC amplitude of 10 mV rms, were employed in all measurements. The electrochemical cell consisted of a lead strip counter electrode, a calomel reference electrode, and a miniaturised lead/acid battery working electrode. All EIS measurements were performed at 25 ^{o}C.

1.4 Timing of the Project

The official contract for Project B23 - Extension of the life and enhancement of the energy density of maintenance-free lead/acid batteries includes the timetable presented in Table 2:

Table 2. Proposed timing of the project over 1997 to 1998.

Battery Making	Dec.			
3 cells tested	Dec. - Feb.			
Cell autopsies		Mar.		
3 cells tested		Mar. - May		
Scientific Paper		Mar. - May		
Cell autopsies			June	
3 cells tested			June - Aug.	
Draft Patenting			June - Aug.	
Cell autopsies				Sept.
3 cells tested				Sept. - Nov.
Technology Transfer				Sept. - Nov.

1.5 Project Results

Seven treated and seven untreated 2 V cells were prepared using as received grids and grids that had been etched in 10 %(w/v) sodium hydroxide, respectively. The formed cells were subjected to charge/discharge cycling using the Australian Standard Traction Battery test. The average discharge capacity data (in Ah kg^{-1}) are presented in Figure 1.

Figures 2(a) and 2(b) present backscattered SEM micrographs for treated and untreated positive plates at the end of the Australian Standard Traction Battery test, respectively. Note that these images were acquired at a magnification of 2000X, and results for other plates are not shown because they are identical to those presented in Figure 2.

Table 3 presents XRD phase compositions for untreated (i.e., plates 62, 67, 69 and 73) and treated (i.e., plates 66, 68, 70, 72 and 74) plates at the end of the Australian Standard Traction Battery test.

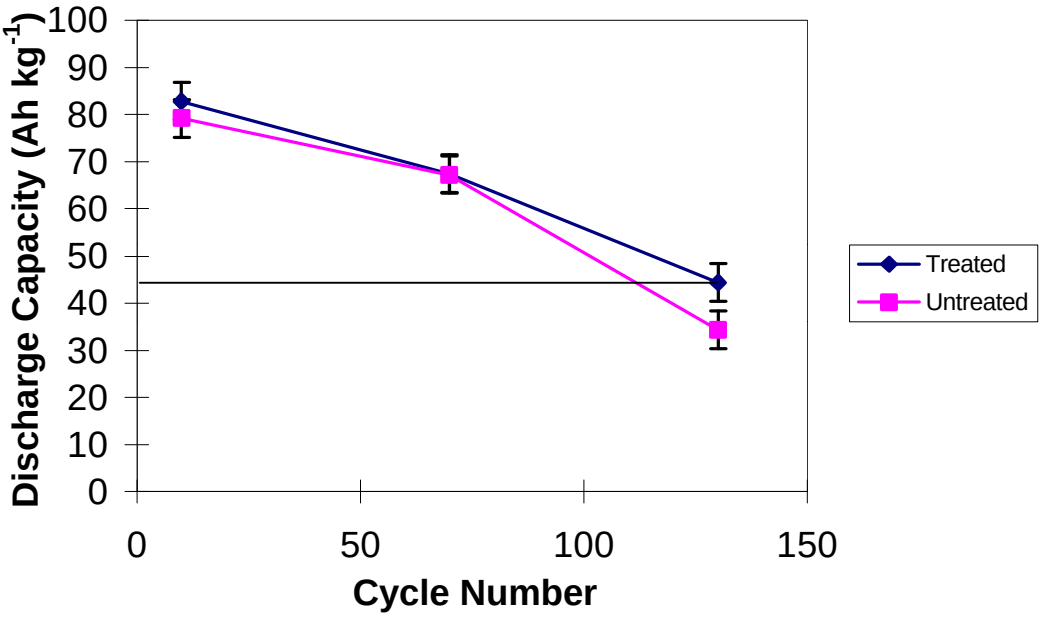

Figure 1 Average discharge capacity data (Ah kg^{-1}) for 2 V cells (7 treated and 6 untreated) that have been tested using the Australian Standard Traction Battery test.

Table 3 XRD phase compositions for positive active materials at the end of the Australian Standard Traction Battery test.

Plate No	% β-PbO_2	% $PbSO_4$
62U	97.18	2.82
66T	98.23	1.77
67U	98.04	1.96
68T	97.09	2.72
69U	91.58	8.42
70T	94.16	5.84
72T	94.61	5.39
73U	91.91	8.09
74T	84.89	15.11

Figures 3(a) and 3(b) present backscattered SEM micrographs for untreated and treated battery cells at the completion of charge/discharge cycling, respectively. EPMA chemical maps for S Kα and Pb Lα X-rays are also presented in Figures 4(a) and 4(b) along with Figures 5(a) and 5(b) for failed untreated and treated positive battery plates, respectively.

Figures 6(a) and 6(b) present secondary ESEM micrographs for as received and sodium hydroxide etched grids. Note that the images in Figures 6(a) and 6(b) were acquired at a magnification of 2000X.

Figure 7 presents a Nyquist plot of imaginary impedance (Z") versus real impedance (Z') for a miniaturised lead/acid battery electrode in battery electrolyte (i.e., 5 M sulfuric acid). Note that the EIS spectra are representative of the naturally occurring electrochemical process in the lead/acid battery as a minimal perturbation of ± 10 mV amplitude is applied to the working electrode.

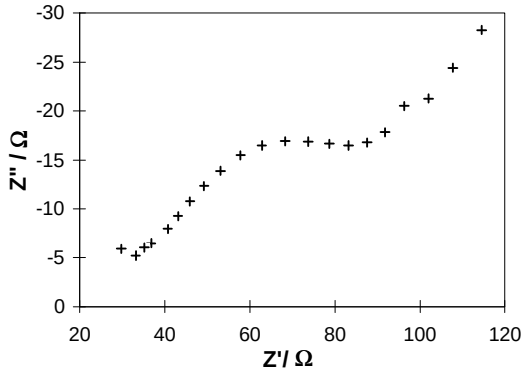

Figure 7 EIS Nyquist plot for a miniaturised lead/acid battery electrode.

Figure 8 presents a schematic diagram of a positive plates showing locations that were sampled, ground and combined in a quality control experiment to verify the reproducibility of the battery production process, and Figures 9(a) and 9(b), respectively, show XRD phase compositions for cured and formed plates that were taken from different paste runs.

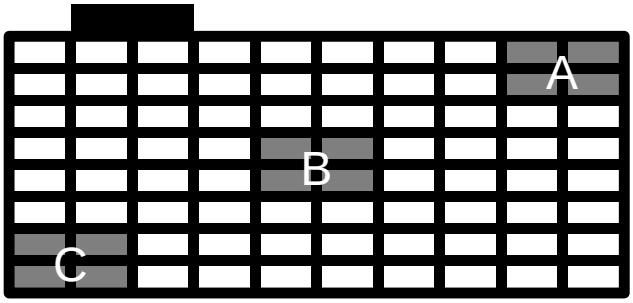

Figure 8 Schematic diagram showing the sampling scheme employed in the quality control experiment for cured and formed plates.

(a)

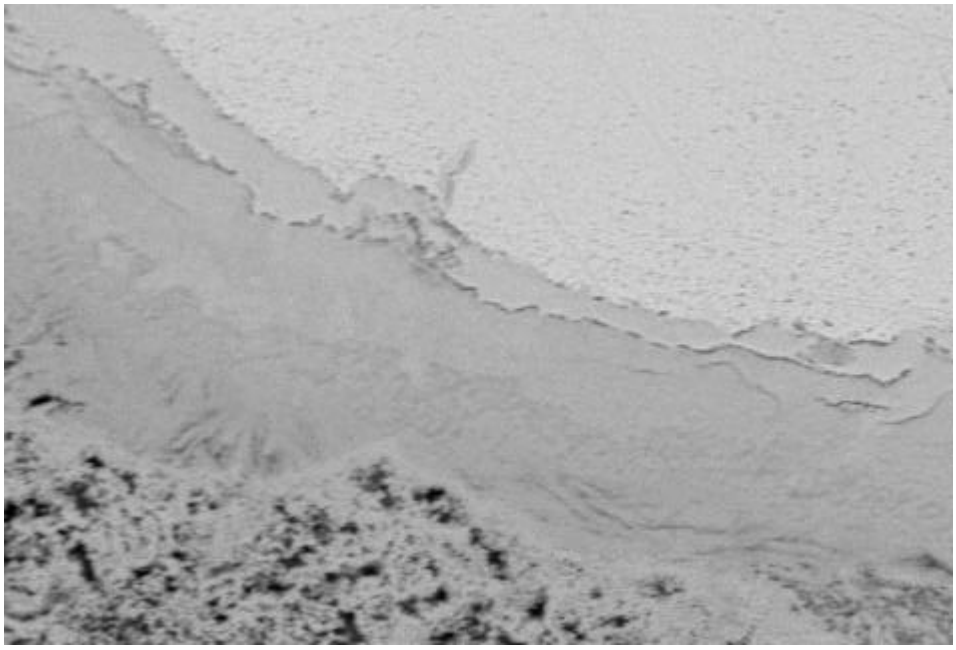

(b)

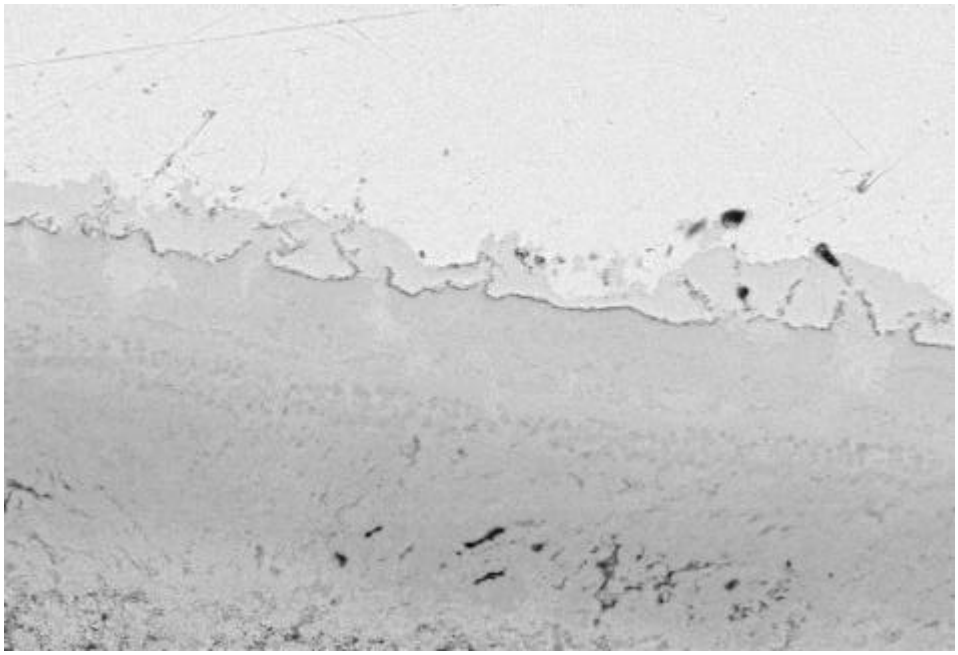

Figure 2 SEM backscattered electron micrographs (magnification = 2000X) of positive plates at the end of the Australian Standard Traction Battery test: (a) a battery grid etched in 10 %w/v sodium hydroxide and (b) an untreated battery grid.

(a)

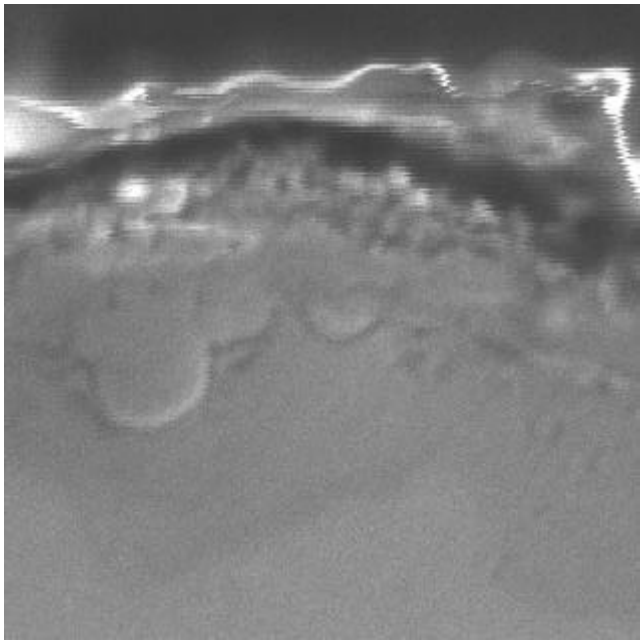

(b)

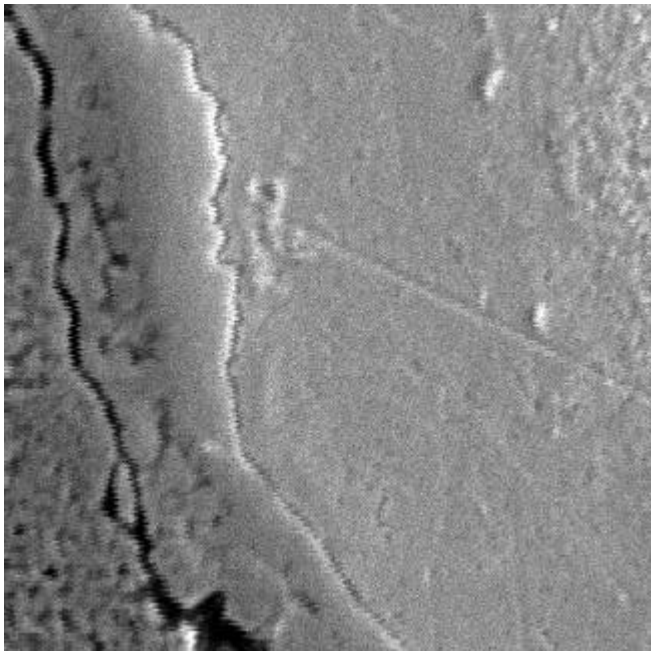

Figure 3 SEM backscattered electron micrographs (magnification = 1000X) of polished cross-sections of positive lead/acid battery plates at the end of charge/discharge cycling using the accelerated charge/discharge cycling regime described elsewhere by De Marco and Jones (November 1997): (a) untreated; (b) treated.

(a)

(b)

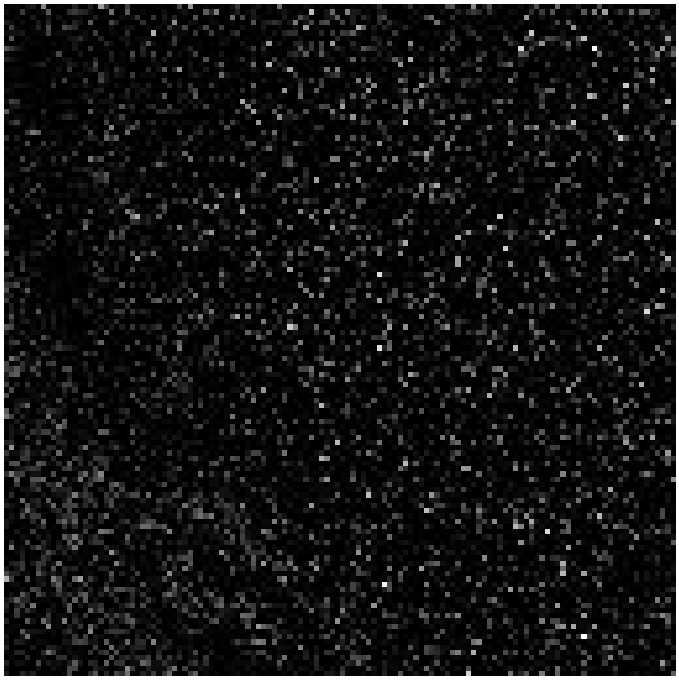

Figure 4 EPMA S Kα X-ray chemical maps for (a) untreated and (b) treated plates shown in Figures 3(a) and 3(b).

(a)

(b)

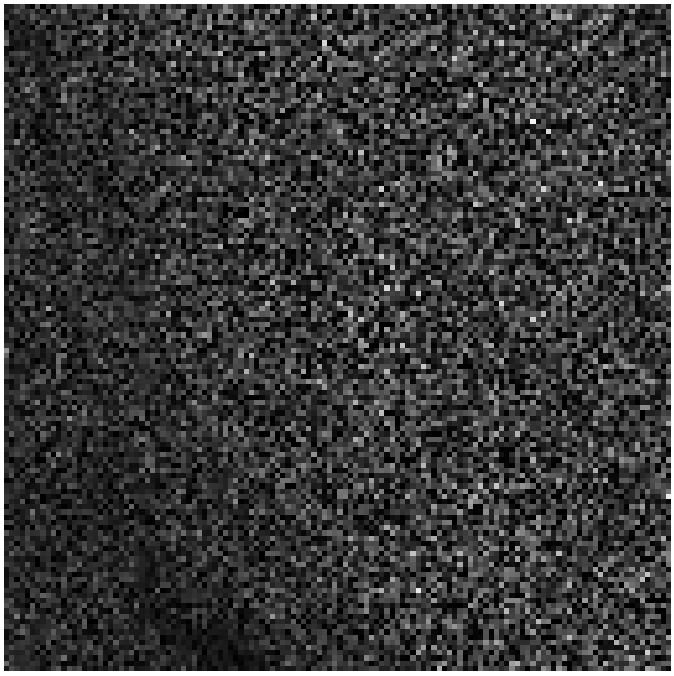

Figure 5 EPMA Pb Lα X-ray chemical maps for (a) untreated and (b) treated plates shown in Figures 3(a) and 3(b).

(a)

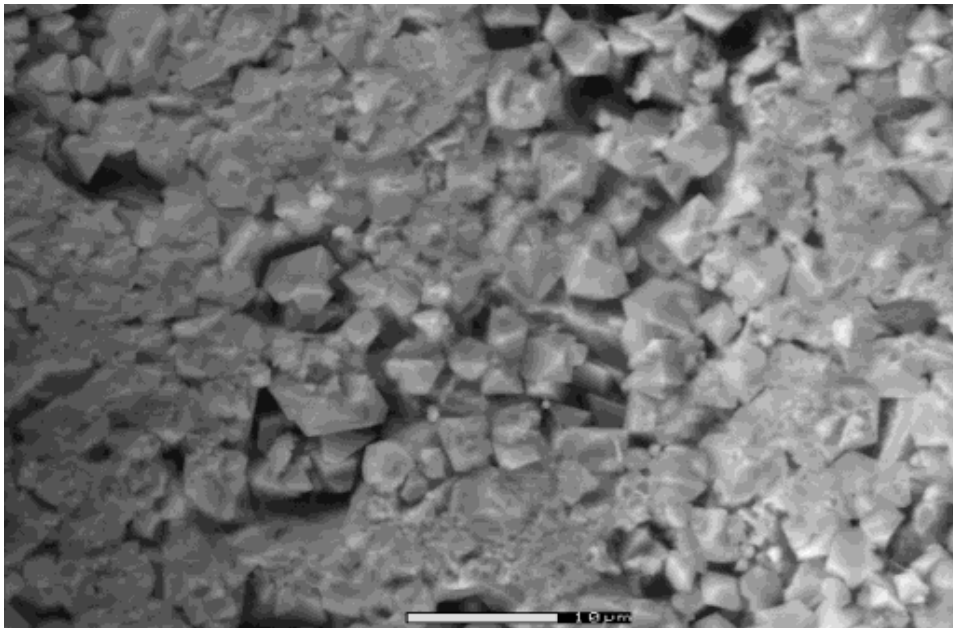

(b)

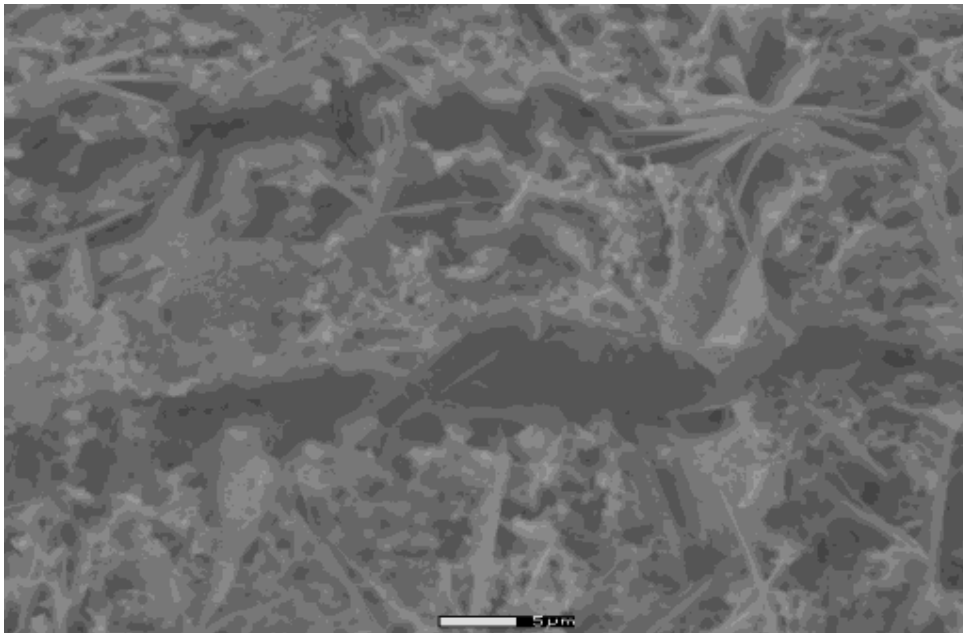

Figure 6 ESEM backscattered electron micrographs (magnification = 2000X) of (a) as received lead/acid battery grid and (b) a battery grid etched in 10 %w/v sodium hydroxide.

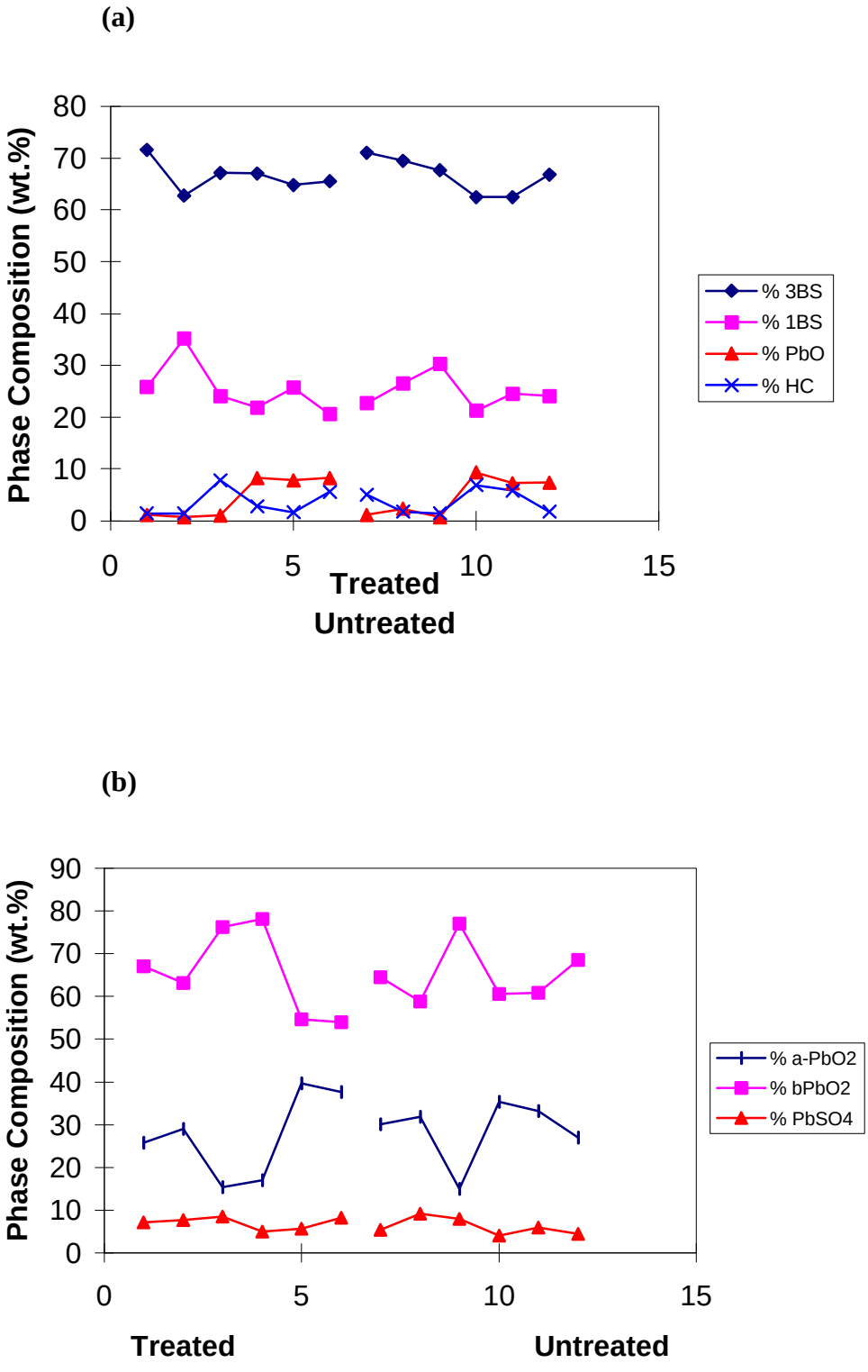

Figure 9 XRD phase compositions of various cured (a) and formed (b) plates produced in different batches.

2 Main Body

2.1 Discussion of the Results

2.1.1 Australian Standard Traction Battery Test

It can be seen in Figure 1 that grid etching in 10%(w/v) sodium hydroxide has no impact on the cycling performance of maintenance-free lead/acid batteries in the initial stages of cycling (i.e., 0 - 60 cycles) under the realistic cycling conditions of the Australian Standard Traction Battery test. Despite this apparent lack of response, it is evident that capacity loss is reduced by 33% for etched grids in the later stages of cycling. Overall, the cycling data shows that an extra 20 cycles are required for etched grids to reach 50% of initial discharge capacity, representing an 18% improvement in battery durability (see the horizontal line in Figure 1).

2.1.2 Characterisation of Failed Battery Plates

A visual inspection of positive battery plates at the end of the Australian Standard Traction Battery test have indicated that active material shedding partly contributed to battery failure. As expected, XRD data for failed plates (see Table 3) demonstrated that cycled battery plates comprise an active material that consists predominantly of β-PbO_2. The presence of low amounts of lead sulfate in active materials of failed positive plates demonstrates that sulfation of active material is not responsible for battery failure. Significantly, the backscattered SEM micrographs presented in Figure 2 show that grid corrosion is the predominant cause of battery failure, as evidenced by the presence of an underlayer film of an insulating material, probably comprising lead sulfate and/or lead monoxide.

Previous SEM work by De Marco and Jones (November 1997) suggested that removal of hydrocerussite by grid etching in sodium hydroxide promotes the formation of a dense corrosion layer of conducting lead dioxide, while untreated grids produce porous corrosion layers that permit the penetration of sulfuric acid and the formation of an underlayer deposit of insulating lead sulfate. Regrettably, energy dispersive X-ray analysis is unable to differentiate between lead sulfate and lead dioxide as the severe

overlap of Pb Lα and S Kα X-ray peaks cannot be resolved. This negative outcome prompted an EPMA study using wavelength dispersive X-ray spectrometers that are capable of resolving the Pb Lα and S Kα X-ray peaks.

The backscattered electron micrograph for an untreated grid [see Figure 3(a)] reveals an irregular underlayer deposit of material at the interface between the grid corrosion layer and grid metal. The EPMA S Kα X-ray chemical map [see Figure 4(a)] clearly shows a predominance of sulfur bearing material in the irregular underlayer deposit. Note that white spots indicate a high concentration of sulfur, while dark regions symbolise a low concentration of sulfur. The accompanying Pb Lα chemical map [see Figure 5(a)] shows that, as expected for lead sulfate, a high level of lead is associated with a high level of sulfur. By contrast, the EPMA S Kα and Pb Lα chemical maps for a treated grid [see Figures 4(b) and 5(b) respectively] display little variation in chemical composition from the porous active material to the corrosion layer and the grid [i.e., left to right profiles in Figures 4(b) and 5(b)], noting that S Kα signals were barely detectable above the background signal. This is due to the fact that the surfaces of all zones are uniform [i.e., the porous active material and corrosion layers are both composed of predominantly lead dioxide along with traces of lead sulfate, while the lead grid surface is fully oxidised (in the first few nanometres) to lead monoxide and/or lead dioxide].

2.1.3 Environmental Scanning Electron Microscopy (ESEM)

Previous unpublished XPS results (De Marco, 1992) demonstrated that grid etching in 10 %w/v sodium hydroxide removes all grid surface hydrocerussite. This work was conducted necessarily under ex situ and ultra-high-vacuum conditions using samples that had been rinsed in distilled water, and these conditions do not mimic those of the wet grid surfaces that are encountered during plate pasting. By contrast, ESEM is capable of providing high resolution images of wet surfaces that are indeed representative of the grid surfaces encountered during plate pasting.

The secondary electron micrograph for an as received grid [see Figure 6(a)] revealed crystalline deposits of detrimental hydrocerussite, while the sodium hydroxide etched specimen [see Figure 6(b)] revealed the roughened grid topography that develops

after dissolution of the crystalline deposits of grid hydrocerussite in 10 %w/v sodium hydroxide.

2.1.4 Electrochemical Impedance Spectroscopy (EIS)

An EIS Nyquist plot reveals semicircles corresponding to interfacial resistive components that reflect the electrochemical behaviour of the working electrode. The EIS spectrum for a miniaturised lead battery electrode (see Figure 7) reveals a low frequency semicircle that is attributable to the charge transfer impedance (i.e., R_{CT}) which is representative of the rate of the electrochemical reaction. The near straight line at 45 degrees at very low frequencies is attributable to a significant diffusional resistance that is better known as the Warburg impedance (i.e., W).

2.1.5 Quality Control of Battery Production Process

Several batches of cured and formed plates were prepared according to the procedures presented in Sections 1.3.1 to 1.3.3. The plates were sampled at the locations shown in Figure 8, mixed and ground to produce one sample per plate for XRD phase analysis. It can be seen in Figure 9 that the XRD phase composition of cured plates is very uniform, while the formed plates show some variation in the ratio of α-PbO_2-to-β-PbO_2 and little variation in $PbSO_4$ content. Note that $PbSO_4$ only arises if the formation of plates is incomplete, so the results in Figure 9(b) signify that formation has gone to completion. Consequently, the plate preparation process is capable of producing reproducible plates of high integrity.

2.1.6 Selected Area X-ray Photoelectron Spectroscopy (XPS)

A scientific paper describing the XRD, SEM and selected area XPS analyses of corrosion layers in lead/acid batteries has been drafted, and will be submitted to the Editorial Office of the Journal of Applied Electrochemistry in late January or early February.

2.1.7 Draft Patenting

Dr. De Marco is presently liaising with the Office for Research and Development at Curtin University of Technology to devise a strategy for commercialisation of the caustic soda etching process that enhances the performance of maintenance-free lead/acid batteries. Dr. Glover, Director of the Office for Research at Curtin University, is presently formulating a strategy for commercialisation of the novel battery production process developed in this work.

3 Conclusion

3.1 Research Findings and their Significance

Results for 7 untreated and 7 treated 2 V cells using the Australian Standard Traction Battery test have demonstrated that grid etching in sodium hydroxide increases the life-time of maintenance-free lead/acid batteries by approximately 18%. These results corroborate the findings of previous research by De Marco and Jones (November, 1997) that were performed using a charge/discharge cycling regime that accelerated battery failure, accentuating the beneficial effects of grid etching in sodium hydroxide.

Autopsies of active materials and grid corrosion layers in positive plates at the end of the Australian Standard Traction Battery test have shown that the major cause of battery failure is grid corrosion. This demonstrates that grid etching in sodium hydroxide is able to ameliorate the detrimental influence of hydrocerussite on grid corrosion and its concomitant effect on battery durability.

EPMA results have detected underlayer deposits of lead sulfate in the corrosion layers of untreated grid positive plates due to the poor adhesion of active material to grids possessing detrimental hydrocerussite. By contrast, the treated grids produce uniform grid corrosion layers consisting predominantly of conducting lead dioxide. Although the preliminary EPMA findings are equivocal, the results are promising enough to warrant further investigation.

ESEM results for wet lead grids etched in 10 %w/v sodium hydroxide proved unequivocally that the alkaline grid pretreatment removes detrimental grid hydrocerussite from the surface of non-antimonial grids. This confirms that the alkaline treatment not only removes hydrocerussite, but prevents it from reforming at a wet grid surface which is exposed to air prior to the pasting of plates.

The Project Team has developed miniaturised lead/acid battery electrodes and an EIS measurement protocol that is suitable for a study of the electrochemistry of the lead/acid battery system. The preliminary data demonstrate that EIS is able to provide critical information pertaining to the kinetics and reaction mechanism of the lead/acid battery. To the best of our knowledge, the chemistry of the lead/acid battery is yet to be studied using EIS.

4 Future Work

The EPMA findings on underlayer deposits of lead sulfate in the corrosion layers of failed lead/acid battery plates will be corroborated by carrying out detailed studies on further specimens.

EIS studies of miniaturised lead/acid battery electrodes at different stages of charge/discharge cycling will be undertaken to gain further insights into the mechanistic chemistry of the lead/acid battery system. Unfortunately, we are yet to develop a protocol for executing charge/discharge cycling and EIS under automatic control, and this aspect is being developed by a Casual Research Assistant working on the Project over the 1998/1999 summer vacation.

5 Acknowledgements

The authors thank GNB Battery Technologies for providing the battery materials used in this study, and the Australian Research Council for additional financial assistance.

6 References

De Marco, R. (1992). X-ray photoelectron spectroscopy results for aged non-antimonial grids that had been etched in 10%(w/v) sodium hydroxide for 10 minutes. unpublished findings.

De Marco, R. (1997). Influence of lead(II) carbonate films of non-antimonial grids on the deep discharge cycling behaviour of maintenance-free lead/acid batteries. Journal of Applied Electrochemistry, 27: 93-98.

De Marco, R. and Jones, J. (1997). Extension of the life and enhancement of the energy density of maintenance-free lead/acid batteries. AEDB Quarterly Report, May: 1-12.

De Marco, R. and Jones, J. (1997). Extension of the life and enhancement of the energy density of maintenance-free lead/acid batteries. AEDB Quarterly Report, November: 1-34.

Manders, J.E., Lam, L.T., De Marco, R., Douglas, J.D., Pillig, R. and Rand, D.A.J. (1994). Battery performance enhancement with additions of bismuth. Journal of Power Sources, 48: 113-128.